Effect of Nuclear Thermal Propulsion Engine Thrust and I_{sp} Tradeoffs and Alternate Propellants on ΔV Budget and Architecture Mass for Crewed Mars Vehicles

Daria Nikitaeva[1], Sean J. Greenhalge[2], Matthew Duchek[3]

[1] *Aerospace Systems Engineer, Advanced Projects, Analytical Mechanics Associates, Huntsville, AL, 35806*

[2] *Project Engineer, Advanced Projects, Advanced Projects, Analytical Mechanics Associates, Denver, CO, 80211*

[3] *Aerospace Engineering Manager, Advanced Projects, Analytical Mechanics Associates, Denver, CO, 80211*

This paper will provide an overview of a spacecraft architecture model developed at AMA as well as an insight into some of the results provided. Currently, preliminary analysis has been completed with this model on evaluating different thrust to weight ratios of Nuclear Thermal Propulsion based vehicles using hydrogen as the propellant by altering the number of engines in the engine block. Gravity losses are incorporated into this analysis as different thrust to weight ratios will provide different burn times. So far, this analysis has shown that in terms of the vehicle mass, it is best to trade the gravity losses for lower vehicle mass as the engines considered add significant dry mass to the vehicle. The final version of this paper will compare gravity losses and vehicle masses for vehicles using different engine masses as well as the ammonia propellant.

I. INTRODUCTION/BACKGROUND

Nuclear Thermal Propulsion (NTP) is an in-space propulsion method which underwent significant development in the United States 1950s through the early 1970s during the Project Rover and Nuclear Engine for Rocket Vehicle Application (NERVA) programs. The goal of these two programs was to create a propulsion system capable of transporting humans to Mars and provide a reusable Lunar shuttle. Unlike chemical propulsion, NTP does not depend on combustion of an oxidizer and fuel to produce thrust; instead, a propellant is pumped into a nuclear reactor and heated to high temperatures before being expelled through a nozzle. Essentially, the NTP-based engine is a monopropellant system [1]. This allows for the theoretical use of any fluid to be used as a propellant if it is compatible with the neutronics inside the reactor and the materials do not exhibit significant degradation throughout the useful life of the engine at the high temperatures and pressures that are typically found inside the reactor core.

Hydrogen is commonly considered as a propellant for NTP engines due to its low molecular weight which maximizes the benefit of the monopropellant capability by maximizing the achievable specific impulse (a measure of propellant efficiency in rocket engines). Hydrogen-based NTP engines in literature have been referred to as H-NTP. Although hydrogen has some favorable properties such as very low molecular weight and a critical point with relatively low pressure and temperature (1.3 MPa and 33 K, respectively), it has high specific heat capacity and low density. These properties exhibit drawbacks in both an engine and space transportation vehicle context, respectively.

An alternate propellant-based NTP (A-NTP) engine was considered by previous work to address hydrogen's high specific heat capacity and low density recommended using anhydrous ammonia as the propellant [2]. This fluid is around ten times denser than hydrogen and has a

specific heat capacity around seven times less than hydrogen. However, ammonia has a molecular weight of 17.031 g/mol which is significantly higher than hydrogen's of 2.016 g/mol resulting in a predicted specific impulse of about 40% that of hydrogen [3]. Although an ammonia-based vehicle architecture results in a comparatively much heavier wetted mass than a hydrogen-based architecture, for certain missions, the storability of the propellant and the reduction in the overall vehicle dry mass may outweigh the wetted mass penalty [4]. Special considerations should be made to accommodate the variations in the burn time by using a finite burn approach which would then lead to the consideration of gravity losses. This paper overviews the models used for vehicle performance estimation and the analysis that is made possible using these models.

II. SPACECRAFT ARCHITECTURE MODEL OVERVIEW

The methodology employed for evaluating NTP vehicle architectures begins with determining the mission architecture along with the required ΔV, typically modeled in Copernicus [5]. Engine performance estimates were obtained from a modular, propellant and cycle flexible high fidelity engine model coded in Simulink with coupled neutronics through OpenMC called the X-NTP model which was documented in detail in previous work [2,6]. This model is capable of not only providing steady state performance metrics but also psuedotransient engine performance parameters that can be made to be functions of any other one parameter that is outputted from the model. When the psuedotransient performance database is coupled with temporal derivatives or relations between parameters, the psuedotransient database yields transient engine performance which could be used inside an Architecture model which is used to simulate and optimize the spacecraft and its architecture given a set of mission specified ΔV values, payload drop schedule, and psuedotransient engine parameter datasets as well as specified vehicle structure and methods of optimization [7]. Further development of this model includes a Master Equipment List (MEL) that scales according to the stage size and launch vehicles considered. This paper provides a detailed walkthrough of the MEL-integrated Architecture model which is then used to perform decoupled gravity loss analysis through Copernicus and compares hydrogen and ammonia propellants in the context of a 2039 Mars Opposition class mission. A comparison without considering gravity losses between hydrogen and ammonia is also made within the context of a 2033 Mars Conjunction class mission to show the differences in vehicle performance for significantly different total mission ΔV values.

II.A. Master Equipment List Physics Models

The Master Equipment List (MEL) is coded in MATLAB and has several modules that support the calculations of the structural/dry mass of the vehicle. The modules that support the MEL can be broken down into two types: (1) Physics Calculations and (2) Constants/Assumptions set up. The MEL then incorporates these separate modules into a coherent model that runs optimization based on the launch vehicle selection and orbit. This section breaks down these modules and describes them followed by a description of their integration and use in the Architecture model.

II.A.1 Battery

The battery mass module takes the required power draw P_{req} and sizes the battery accordingly to obtain the mass of the batteries m_{bat}. The first calculation is the determination of the total degradation factor D_F based on the degradation rate D_R and the lifetime l of the battery via . Using D_F, the useable capacity E_{use} can be found from P_{req}, power margin P_{mar}, battery efficiency η_{bat}, and the number of batteries n_{bat} through the relation shown in . Then the total

capacity E_{tot} is found by incorporating the battery discharge depth d_d as shown in . The power density ρ_{pwr}, which is the power per kilogram, is then used to find m_{bat} as shown in . The assumed power densities and battery types that are implied are shown in **Error! Reference source not found.**.

Table 1: Battery Types and Power Densities

Battery Type	Power Density (W-hr/kg)
Ni-CD	30
Ni-H2	60
Li-ion	125

$$D_F = \left(1 - \frac{D_R}{100}\right)^l \quad \text{Eq. 1}$$

$$E_{use} = \frac{P_{req}(1 + P_{mar})}{\eta_{bat} D_F n_{bat}} \quad \text{Eq. 2}$$

$$E_{tot} = \frac{E_{use}}{d_d} \quad \text{Eq. 3}$$

$$m_{bat} = \frac{E_{tot}}{\rho_{pwr}} n_{bat} \quad \text{Eq. 4}$$

II.A.2 Bus Structure

The Bus Structure module is assumed to be the skirt that extends beyond the propellant tank and houses various components for that stage with a single output that provides the mass of the bus structure m_{bus}. The arguments that this module accepts are the launch vehicle selection and number of docking ports. The bus structure is modeled as a solid body made of a selected material (or a structure with openings and an average density) in the shape of an open cylinder without end caps. The volume is found by using an assumed thickness thin-shelled cylinder which can be converted into mass through a material density. Furthermore, if a stage docks at both ends, there is a cylindrical bus at both ends and vice versa.

II.A.3 Communications/Command & Data-Handling Systems/Guidance, Navigation, & Control

The Communications/Command & Data-Handling Systems/Guidance, Navigation, & Control (C/CDH/GNC) module simply loads the setup parameters for the different components and sums the different power levels to get the total power required. For the masses, each mass $m_{\mathrm{C/CDH/GNC}_i}$ is modified by the mass growth allowance MGA_i (in percent) for each individual component and all of them are summed together for the total mass of this system $m_{\mathrm{C/CDH/GNC}_{tot}}$ as shown in SEQ Equation * MERGEFORMAT .

$$m_{\mathrm{C/CDH/GNC}_{tot}} = \sum_{i=1}^{n} \left[m_{\mathrm{C/CDH/GNC}_i} \left(1 + \frac{MGA_i}{100}\right) \right] \quad \text{Eq. 5}$$

II.A.4 Cryogenic Fluid Management

The Cryogenic Fluid Management (CFM) module determines not only the mass m_{CFM} but also the power $\dot{W}_{CFM}$ and heat $\dot{Q}_{CFM}$ that must be rejected by the radiators given the tank surface area $A_{s_{tank}}$ and the CFM configuration CFM_{config} (can be active, passive, or reduced boil-off) as the inputs. The raw heat rejected $\dot{Q}_{rej}$ and required power for the cryocoolers (CC) at specified temperatures $\dot{W}_{req_T}$ is calculated by SEQ Equation * MERGEFORMAT and SEQ Equation * MERGEFORMAT , respectively which are based on the CC lifts at a temperature L_T and the input power to provide that lift at that temperature $\dot{W}_{L_T}$. The masses of the secondary structures, multi-insultation layer (MLI), spray-on foam insulation (SOFI), and structural MLI are calculated using the setup parameters for CFM. The secondary structure mass m_{SS} considers the CC mixers m_{mix} and sensors $m_{sensors}$ as well as the radio frequency mass gauging (RFMG) m_{RFMG} and tank support MLI m_{TSMLI} with the formulation shown in SEQ Equation * MERGEFORMAT . The mass of the actual MLI m_{MLI} is determined by the number of MLI layers n_{MLI}, specific mass of each MLI layer $m_{sp_{MLI}}$ in $\mathrm{kg/m^2}$, and $A_{s_{tank}}$ as shown in SEQ Equation * MERGEFORMAT . The mass of SOFI m_{SOFI} is determined by the thickness of SOFI t_{SOFI}, density of SOFI ρ_{SOFI}, and $A_{s_{tank}}$ which is shown in SEQ Equation * MERGEFORMAT . The structural MLI mass $m_{MLI_{struct}}$ depends on the number of structural MLI layers $n_{MLI_{struct}}$, specific mass of the structural MLI $m_{sp_{MLI_{struct}}}$ in $\mathrm{kg/m^2}$, and $A_{s_{tank}}$ which is shown in SEQ Equation * MERGEFORMAT .

$$\dot{Q}_{rej} = \sum_{T=T_1}^{n} (L_T) \quad \text{Eq. 6}$$

$$\dot{W}_{req_T} = \sum_{T=T_1}^{n} \left(L_T \dot{W}_{L_T}\right) \quad \text{Eq. 7}$$

$$m_{SS} = m_{RFMG} + m_{mix} + m_{sensors} + m_{TSMLI} \quad \text{Eq. 8}$$

$$m_{MLI} = n_{MLI} m_{sp_{MLI}} A_{s_{tank}} \quad \text{Eq. 9}$$

$$m_{SOFI} = t_{SOFI} A_{s_{tank}} \rho_{SOFI} \quad \text{Eq. 10}$$

$$m_{MLI_{struct}} = n_{MLI_{struct}} m_{sp_{MLI_{struct}}} A_{s_{tank}} \quad \text{Eq. 11}$$

The CC masses, $\dot{W}_{CFM}$, and $\dot{Q}_{CFM}$ are calculated using specific correlations in a switch case that is based on CFM_{config}.

II.A.4.i Active

The CC mass m_{CC} is determined by the CC specific mass at a temperature m_{sp_T}, L_T, and the CC redundancy R_{CC} as shown in SEQ Equation * MERGEFORMAT . The mass of the broad area cooling (BAC) m_{BAC} is dependent on the areal tube density of the tubes inside the tank ρ_{t_i}, the tube and shield areal density outside the tank ρ_{st_o}, and $A_{s_{tank}}$ which is shown in SEQ Equation * MERGEFORMAT . The total power of the active CFM $\dot{W}_{CFM}$ is provided by the summation of the different required powers at specified temperatures $\dot{W}_{req_T}$ as shown in SEQ Equation *

MERGEFORMAT . The total heat that is required to be rejected by the radiators from the CC $\dot{Q}_{CFM}$ is the summation of $\dot{W}_{CFM}$ and $\dot{Q}_{rej}$ as shown in SEQ Equation * MERGEFORMAT .

$$m_{CC} = \sum_{T=T_1}^{n} \left(m_{sp_T} L_T R_{CC}\right) \quad \text{Eq. 12}$$

$$m_{BAC} = \left(\rho_{t_i} + \rho_{st_o}\right) A_{s_{tank}} \quad \text{Eq. 13}$$

$$\dot{W}_{CFM} = \sum_{T=T_1}^{n} \left(\dot{W}_{req_T}\right) \quad \text{Eq. 14}$$

$$\dot{Q}_{CFM} = \dot{W}_{CFM} + \dot{Q}_{rej} \quad \text{Eq. 15}$$

II.A.4.i Passive

This mode returns a CFM mass, power, and heat rejected as 0.

II.A.4.i Reduced Boil-Off

This mode limits the temperatures that are used in the CFM and calculates the mass based on the higher temperature CFM using SEQ Equation * MERGEFORMAT through SEQ Equation * MERGEFORMAT .

II.A.5 Engine

The engine component calculates the total mass of the engine m_{eng} as well as the electrical power requirements given engine subcomponent masses, start up/shut down times, and burn time lengths. The average power required for engine operations $\dot{W}_{avg}$ are based on the engine peak and idle power ($\dot{W}_{peak}$ and $\dot{W}_{id}$), time at peak and idle power (t_{peak} and t_{id}), and the number of burns n_{burn} with the relation shown in SEQ Equation * MERGEFORMAT . The energy of each burn E_{burn} depends on $\dot{W}_{peak}$; start up, steady state, shut down, and cooldown times (t_{su}, t_{ss}, t_{sd}, and t_{cd}); start up, steady state, shut down, and cooldown power factors (f_{su}, f_{ss}, f_{sd}, and f_{cd}) as shown in SEQ Equation * MERGEFORMAT . The idle energy E_{id} required is based on t_{id} and $\dot{W}_{id}$ as shown in SEQ Equation * MERGEFORMAT . The single burn cycle energy E_{cycle} is summation of E_{burn} and E_{id} as shown in SEQ Equation * MERGEFORMAT and the total mission energy $E_{mission}$ depends on E_{cycle}, n_{burn}, and number of engines n_{eng} as shown in SEQ Equation * MERGEFORMAT . The total burn time t_{burn} depends on t_{su}, t_{ss}, t_{sd}, and t_{cd} as shown in SEQ Equation * MERGEFORMAT . The burn power required $\dot{W}_{burn}$ to operate all the engines depends on E_{burn}, t_{burn}, and n_{eng} as shown in SEQ Equation * MERGEFORMAT .

$$\dot{W}_{avg} = \frac{\dot{W}_{peak} t_{peak} n_{burn} + \dot{W}_{id} t_{id}}{t_{peak} + t_{id}} \quad \text{Eq. 16}$$

$$E_{burn} = \dot{W}_{peak}(f_{su} t_{su} + f_{ss} t_{ss} + f_{sd} t_{sd} + f_{cd} t_{cd}) \quad \text{Eq. 17}$$

$$E_{id} = \dot{W}_{id} t_{id} \quad \text{Eq. 18}$$

$$E_{cycle} = E_{id} + E_{burn} \quad \text{Eq. 19}$$

$$E_{mission} = \left(E_{cycle} n_{burn} + E_{id}\right) n_{eng} \quad \text{Eq. 20}$$

$$t_{burn} = t_{su} + t_{ss} + t_{sd} + t_{cd} \quad \text{Eq. 21}$$

$$\dot{W}_{burn} = \frac{E_{burn}}{t_{burn}} n_{eng} \quad \text{Eq. 22}$$

The total engine mass m_{eng} is the summation of user defined subcomponent masses which include the reactor $m_{reactor}$, engine hardware $m_{hardware}$, nozzle m_{nozzle}, nozzle extension m_{ext}, propellant ducting m_{duct}, external shield m_{shield}, and n_{eng} as shown in SEQ Equation * MERGEFORMAT .

$$m_{eng} = (m_{reactor} + m_{hardware} + m_{nozzle} + m_{ext} + m_{duct} + m_{shield}) n_{eng} \quad \text{Eq. 23}$$

II.A.6 Docking and Thrust Structure

The docking and thrust structure modules calculate the mass of the connecting beams that hold the structures in place with the spacecraft mass, launch vehicle selection, and number of supported structures as inputs. The lateral loads F_{lat} depend on the spacecraft mass m_{SC}, the maximum lateral G's the launch vehicle will exhibit laterally G_{lat}, and a factor of safety FS as well as the gravitational constant g of 9.807 m/s^2 as shown in SEQ Equation * MERGEFORMAT . The radius of the bus r_{bus} is assumed to be three quarters of the maximum payload radius. Since only the maximum and minimum payload diameters are known, $d_{pay_{max}}$ and $d_{pay_{min}}$, respectively, the bus radius becomes what is shown in SEQ Equation * MERGEFORMAT , which is based on $d_{pay_{max}}$. The assumptions are true for the adapter radius r_{adapt}, except that it uses $d_{pay_{min}}$ as shown in SEQ Equation * MERGEFORMAT . In both SEQ Equation * MERGEFORMAT and SEQ Equation * MERGEFORMAT , the parameter C is a scaling value that has been assumed to be 0.75 for the docking structure and 0.95 for the thrust structure. The length of each beam L_{beam} is determined through trigonometry with the bus height H being the length parameter and the difference between r_{adapt} and r_{bus} being the width parameter as shown in SEQ Equation * MERGEFORMAT through the Pythagorean theorem. The angle that the beam makes with the base of the payload bay θ is dependent on the difference between r_{adapt} and r_{bus} as well as L_{beam} as shown in SEQ Equation * MERGEFORMAT . The lateral force experienced by the beams $F_{beam_{lat}}$ is dependent on F_{lat}, θ, and the difference between r_{adapt} and r_{bus} with the relation shown in SEQ Equation * MERGEFORMAT .

$$F_{lat} = m_{SC} g G_{lat} FS \quad \text{Eq. 24}$$

$$r_{bus} = \frac{d_{pay_{max}}}{2} C \quad \text{Eq. 25}$$

$$r_{adapt} = \frac{d_{pay_{min}}}{2} C \quad \text{Eq. 26}$$

$$L_{beam} = \sqrt{\left(r_{bus} - r_{adapt}\right)^2 + H^2} \quad \text{Eq. 27}$$

$$\theta = \cos^{-1}\left(\frac{r_{bus} - r_{adapt}}{L_{beam}}\right) \quad \text{Eq. 28}$$

$$F_{beam_{lat}} = \frac{F_{lat}}{\left(r_{bus} - r_{adapt}\right)\sin(\theta)} \quad \text{Eq. 29}$$

The axial load from the launch vehicle F_{axial} is determined from m_{SC}, the maximum launch vehicle axial G's G_{axial}, g, and FS as shown in SEQ Equation * MERGEFORMAT . The axial load on the beam $F_{beam_{axial}}$ is dependent on F_{axial}, number of beams n_{beam}, and θ as shown in SEQ Equation * MERGEFORMAT . Notice that $F_{beam_{lat}}$ does not depend on the number of beams as the maximum lateral force would be all the applied force loaded on to one beam. The maximum compressive load on any one beam F_{beam} is the sum of $F_{beam_{axial}}$ and $F_{beam_{lat}}$ as shown in SEQ Equation * MERGEFORMAT . The minimum area that is required per beam A_{beam} is dependent on F_{beam} and the yield strength of the material $\sigma_{Y_{mat}}$ as shown in SEQ Equation * MERGEFORMAT . Assuming that each beam has a circular cross-sectional area, the radius of the beam based on area r_{beam_A} is provided by SEQ Equation * MERGEFORMAT . The second moment of inertia II of the beam is dependent on F_{beam}, ultimate factor of safety UFS, L_{beam}, and the modulus of elasticity of the material E_{mat} as shown in SEQ Equation * MERGEFORMAT . The resulting beam radius from II, $r_{beam_{II}}$, is shown in SEQ Equation * MERGEFORMAT . The maximum beam radius $r_{beam_{max}}$ is selected from r_{beam_A} and $r_{beam_{II}}$. The resulting beam volume $\forall_{beam}$ is determined from $r_{beam_{max}}$ and L_{beam} as shown in SEQ Equation * MERGEFORMAT . The total mass of all the beams for the structure m_{struct} is dependent on $\forall_{beam}$, n_{beam}, and the density of the material ρ_{mat} as shown in SEQ Equation * MERGEFORMAT .

$$F_{axial} = m_{SC} g G_{axial} FS \quad \text{Eq. 30}$$

$$F_{beam_{axial}} = \frac{F_{axial}}{n_{beam} \sin(\theta)} \quad \text{Eq. 31}$$

$$F_{beam} = F_{beam_{lat}} + F_{beam_{axial}} \quad \text{Eq. 32}$$

$$A_{beam} = \frac{F_{beam}}{\sigma_{Y_{mat}}} \quad \text{Eq. 33}$$

$$r_{beam_A} = \sqrt{\frac{A_{beam}}{\pi}} \quad \text{Eq. 34}$$

$$II = \frac{F_{beam} L_{beam}^2 UFS}{2\pi^2 E_{mat}} \quad \text{Eq. 35}$$

$$r_{beam_{II}} = \left(\frac{2II}{\pi}\right)^{1/4} \quad \text{Eq. 36}$$

$$\forall_{beam} = \pi r_{beam_{max}}^2 L_{beam} \quad \text{Eq. 37}$$

$$m_{struct} = \forall_{beam} \rho_{mat} n_{beam} \quad \text{Eq. 38}$$

II.A.7 Main Propellant Tank

The Main Propellant Tank Module considers the length of the different components that contribute to the overall length of the spacecraft such as the engine, bus, and thrust structures and outputs tank parameters such as dry tank mass $m_{tank_{dry}}$, tank surface area $A_{s_{tank}}$, and the total wetted tank mass m_{tank}. The length limit of the spacecraft is the useable payload length of the payload bay of the selected launch vehicle. The tank diameter d_{tank} is the useable payload diameter d_{pay} of the launch vehicle with a specified insultation thickness t_{ins}, that could be

informed by other parameters of CFM, subtracted as shown in SEQ Equation * MERGEFORMAT which can be converted to a tank radius r_{tank}. It is assumed that the tank shape is cylindrical with ellipsoid shaped domes on the ends. The dome height h_{dome} is taken to be a function of r_{tank} and the relation is shown in SEQ Equation * MERGEFORMAT . The volume of the dome $\forall_{dome}$, which is half an ellipsoid, is based on r_{tank} and h_{dome} with the relation shown in SEQ Equation * MERGEFORMAT . The surface area of the dome $A_{s_{dome}}$ is also based r_{tank} and h_{dome} as well as a user defined ellipsoidal parameter p for which the relation is shown in SEQ Equation * MERGEFORMAT .

$$d_{tank} = d_{pay} - 2t_{ins} \rightarrow r_{tank} = \frac{d_{tank}}{2} \quad \text{Eq. 39}$$

$$h_{dome} = \frac{\sqrt{2}}{2} r_{tank} \quad \text{Eq. 40}$$

$$\forall_{dome} = \frac{2}{3} r_{tank}^2 h_{dome} \quad \text{Eq. 41}$$

$$A_{s_{dome}} = 2\pi \left[\frac{1}{3} \left(r_{tank}^{2p} + 2 r_{tank}^{p} h_{dome}^{p} \right) \right]^{1/p} \quad \text{Eq. 42}$$

The total length of the tank L_{tank} is dictated by the payload mass and volume capabilities of the launch vehicle for the selected orbit. A volume limited payload is one that utilizes the entire payload bay length L_{pay} while also accounting for the lengths of other components of the spacecraft such as the bus structure L_{bus}, docking structure L_{dock}, thrust structure L_{thrust}, and engine L_{eng}. Other parameters that dictate how the component lengths are used include the number of docking ports n_{dock} and if the spacecraft has engines (B_{eng}, which is a Boolean operator). All this is put together and shown in SEQ Equation * MERGEFORMAT for the volume limited tank length $L_{tank_{\forall}}$. The tank length of a mass limited payload L_{tank_m} will ALWAYS be lower than or equal to $L_{tank_{\forall}}$ and L_{tank_m} is iteratively adjusted according to the comparison of the launch vehicle payload mass capabilities and the resulting total spacecraft mass as discussed in Section II.B.

$$L_{tank_{\forall}} = L_{pay} - \left[(L_{bus} + L_{dock}) n_{dock} + \left(L_{thrust} + L_{eng} \right) B_{eng} \right] \quad \text{Eq. 43}$$

The length of the cylindrical section of the tank L_{cyl} is based on L_{tank} (generic length, it does not matter if its volume or mass limited) with $2h_{dome}$ subtracted from it as shown in SEQ Equation * MERGEFORMAT . The surface area and volume of the cylindrical section ($A_{s_{cyl}}$ and $\forall_{cyl}$) use the standard cylindrical geometrical equations shown in SEQ Equation * MERGEFORMAT and SEQ Equation * MERGEFORMAT , respectively. The resulting total surface area and volume of the tank ($A_{s_{tank}}$ and $\forall_{tank}$) consist of two domes and the cylinder as shown in SEQ Equation * MERGEFORMAT and SEQ Equation * MERGEFORMAT , respectively.

$$L_{cyl} = L_{tank} - 2h_{dome} \quad \text{Eq. 44}$$

$$A_{s_{cyl}} = 2\pi r_{tank} L_{cyl} \quad \text{Eq. 45}$$

$$\forall_{cyl} = \pi r_{tank}^2 L_{cyl} \quad \text{Eq. 46}$$

$$A_{s_{tank}} = A_{s_{cyl}} + 2A_{s_{dome}} \quad \text{Eq. 47}$$

$$\forall_{tank} = \forall_{cyl} + 2\forall_{dome} \quad \text{Eq. 48}$$

The total propellant mass inside the tank m_{prop} is based on $\forall_{tank}$ and propellant density ρ_{prop} as shown in SEQ Equation * MERGEFORMAT . The usable propellant mass $m_{prop_{use}}$ accounts for the ullage δ_U (units in percent) and the resulting formulation shown in SEQ Equation * MERGEFORMAT .

$$m_{prop} = \forall_{tank}\rho_{prop} \quad \text{Eq. 49}$$

$$m_{prop_{use}} = m_{prop}\left(1 - \frac{\delta_U}{100}\right) \quad \text{Eq. 50}$$

To find the mass of the tank m_{tank}, the thickness of the tank t_{tank} needs to be evaluated which is based on the internal pressure of the tank P_{prop} and the static hydraulic pressure P_{hyd} caused by the launch vehicle acceleration which is characterized by the axial loads G_{axial}. is determined by SEQ Equation * MERGEFORMAT where g is 9.807 m/s^2 and the maximum pressure of the tank P_{max} that will be used in determining the tank thickness is shown in SEQ Equation * MERGEFORMAT . It is assumed that the tank is an isogrid structure and the thickness of the isogrid skin t_{skin} is provided by SEQ Equation * MERGEFORMAT which is based on P_{max}, a factor of safety FS, r_{tank}. yield strength of the material σ_Y, the first non-dimensional iso-grid geometry property α, and the knockdown parameter k which accounts for the added tension in bending from lateral loads. The equivalent weight thickness $\bar{t}$ is provided by SEQ Equation * MERGEFORMAT which provides the thickness of a non-iso-grid tank with the same size and mass as an iso-grid tank and is based on t_{skin}, α, and a second non-dimensional isogrid geometrical property μ which is 0 for an unflanged iso-grid. The dome thickness $\bar{t}_{dome}$ is obtained by scaling $\bar{t}$ by a thickness ratio T_R as shown in SEQ Equation * MERGEFORMAT . The dry mass of the tank $m_{tank_{dry}}$ is found by scaling the surface areas of the cylindrical $A_{s_{cyl}}$ and dome $A_{s_{dome}}$ components of the tank by their respective thicknesses $\bar{t}$ and $\bar{t}_{dome}$ to obtain the volume of the material $\forall_{mat}$ and scaling it by the material density ρ_{mat} as shown in SEQ Equation * MERGEFORMAT . m_{tank} includes $m_{tank_{dry}}$ and m_{prop} as shown in SEQ Equation * MERGEFORMAT .

$$P_{hyd} = L_{tank}\rho_{prop}gG_{axial} \quad \text{Eq. 51}$$

$$P_{max} = P_{prop} + P_{hyd} \quad \text{Eq. 52}$$

$$t_{skin} = \frac{P_{max}r_{tank}FS}{2\sigma_Y k(1+\alpha)} \quad \text{Eq. 53}$$

$$\bar{t} = t_{skin}[1 + 3(\alpha + \mu)] \quad \text{Eq. 54}$$

$$\bar{t}_{dome} = \bar{t}T_R \quad \text{Eq. 55}$$

$$m_{tank_{dry}} = \rho_{mat}\left(A_{s_{cyl}}\bar{t} + 2A_{s_{dome}}\bar{t}_{dome}\right) \quad \text{Eq. 56}$$

$$m_{tank} = m_{tank_{dry}}m_{prop} \quad \text{Eq. 57}$$

II.A.8 Power Management and Distribution (PMAD)

The Power Management and Distribution (PMAD) module depends on the peak power draw $\dot{W}_{peak}$ and outputs the PMAD mass m_{PMAD}, required power $\dot{W}_{req}$, and waste heat $\dot{Q}_{waste}$. The box and cable specific masses, $m_{sp_{box}}$ and $m_{sp_{cable}}$, respectively, are determined by scaling a user defined normalized box mass $\bar{m}_{box}$ and normalized cable mass $\bar{m}_{cable}$ by 0.0105 kg/W as shown in SEQ Equation * MERGEFORMAT and SEQ Equation * MERGEFORMAT , respectively. The box mass per PMAD unit m_{box} is determined from $\dot{W}_{peak}$ and $m_{sp_{box}}$ as shown in SEQ Equation * MERGEFORMAT . Similarly, the cable mass per PMAD unit m_{cable} is dependent on $\dot{W}_{peak}$ and $m_{sp_{cable}}$ as shown in SEQ Equation * MERGEFORMAT . The total PMAD mass m_{PMAD} is then the summation of m_{box} and m_{cable} and is scaled by the number of PMAD units n_{PMAD} as shown in SEQ Equation * MERGEFORMAT . The required power $\dot{W}_{req}$ is dependent on the PMAD efficiency η_{PMAD} and $\dot{W}_{peak}$ as shown in SEQ Equation * MERGEFORMAT . The waste heat $\dot{Q}_{waste}$ is then the difference between $\dot{W}_{req}$ and $\dot{W}_{peak}$ as shown in SEQ Equation * MERGEFORMAT .

$$m_{sp_{box}} = 0.0105\bar{m}_{box} \quad \text{Eq. 58}$$

$$m_{sp_{cable}} = 0.0105\bar{m}_{cable} \quad \text{Eq. 59}$$

$$m_{box} = \dot{W}_{peak} m_{sp_{box}} \quad \text{Eq. 60}$$

$$m_{cable} = \dot{W}_{peak} m_{sp_{cable}} \quad \text{Eq. 61}$$

$$m_{PMAD} = (m_{box} + m_{cable}) n_{PMAD} \quad \text{Eq. 62}$$

$$\dot{W}_{req} = \frac{\dot{W}_{peak}}{\eta_{PMAD}} \quad \text{Eq. 63}$$

$$\dot{Q}_{waste} = \dot{W}_{req} - \dot{W}_{peak} \quad \text{Eq. 64}$$

II.A.9 Radiator and Mechanisms

The radiator depends on the CFM heat rejection $\dot{Q}_{CFM}$ and the waste heat from the PMAD $\dot{Q}_{PMAD_{waste}}$, and it outputs the mass of the radiator panels m_{rad} and the mass of the radiator mechanisms $m_{rad_{mech}}$. A user specified parameter is defined that provides information about if the radiator radiates from only one side or both sides and is used in the calculations as an area modifier A_M of 0.5 for both sides and 1 for a single side. The area of the radiator A_{rad} is determined by the radiative heat transfer equation that is dependent on $\dot{Q}_{CFM}$ and $\dot{Q}_{PMAD_{waste}}$, a factor of safety FS, Stefan-Boltzmann constant of $\sigma = 5.67 \times 10^{-8}$, radiator emissivity ε, radiator temperature that is user specified T_{rad} (future iterations of this module will include a more detailed radiator analysis to remove this assumption), the environmental temperature T_{env} that is typically assumed to be between 3 K and 4 K, and A_M as shown in SEQ Equation * MERGEFORMAT . The mass of the radiator panels m_{rad} is determined by a radiator areal density ρ_{rad} and A_{rad} as shown in SEQ Equation * MERGEFORMAT . To obtain the mass of the radiator mechanisms $m_{rad_{mech}}$, A_{rad} is scaled by 3.4 as shown in SEQ Equation * MERGEFORMAT .

$$A_{rad} = \frac{(\dot{Q}_{CFM} + \dot{Q}_{PMAD_{waste}})FS}{\sigma\varepsilon(T_{rad}^4 - T_{env}^4)} A_M \quad \text{Eq. 65}$$

$$m_{rad} = \rho_{rad} A_{rad} \quad \text{Eq. 66}$$

$$m_{rad_{mech}} = 3.4 A_{rad} \quad \text{Eq. 67}$$

II.A.10 Reaction Control System (RCS)

The Reaction Control System (RCS) module determines the total RCS mass m_{RCS}, wetted mass $m_{RCS_{wet}}$, piping mass $m_{RCS_{pipe}}$, mass of thrusters $m_{RCS_{thrusters}}$, power of thrusters $\dot{W}_{RCS_{thrusters}}$, power for the piping $\dot{W}_{RCS_{pipe}}$, dry mass of the RCS system $m_{RCS_{dry}}$, and the RCS propellant mass $m_{RCS_{prop}}$ given the required RCS ΔV_{RCS} and the mass of the spacecraft m_{SC}. $m_{RCS_{prop}}$ is determined based on the Ideal Rocket Equation, m_{SC}, RCS specific impulse $I_{sp_{RCS}}$, g, and the tank ullage δ_U as shown in SEQ Equation * MERGEFORMAT . A mixture mass ratio ϕ is used to determine the mass of the fuel m_{fuel} and the mass of the oxidizer m_{ox} as shown in SEQ Equation * MERGEFORMAT and SEQ Equation * MERGEFORMAT , respectively. At this point, the calculations split between the fuel and oxidizer, however, they are the same for each fluid.

$$m_{RCS_{prop}} = \left[m_{SC} \exp\left(\frac{\Delta V_{RCS}}{I_{sp_{RCS}} g} \right) \right] (1 + \delta_U) \quad \text{Eq. 68}$$

$$m_{fuel} = \frac{m_{RCS_{prop}}}{1 + \phi} \quad \text{Eq. 69}$$

$$m_{ox} = m_{RCS_{prop}} - m_{fuel} \quad \text{Eq. 70}$$

The mass of fluid per tank $m_{fluid_{tank}}$ is determined by the total mass of the fluid m_{fluid} (m_{fuel} or m_{ox}) and the total number of RCS tanks $n_{RCS_{tank}}$ which include both fuel and oxidizer tanks as shown in SEQ Equation * MERGEFORMAT . The internal volume of the tank $\forall_{in}$ is determined by $m_{fluid_{tank}}$, density of the fluid ρ_{fluid}, and δ_U as shown in SEQ Equation * MERGEFORMAT . Assuming that the tank is a spherical shape, the internal radius of the tank r_{in} is determined by $\forall_{in}$ as shown in SEQ Equation * MERGEFORMAT . The maximum pressure that the tank experiences P_{max} is due the tank stagnation pressure P_0 and axial loads G_{axial} which depend on r_{in} and ρ_{fluid} as shown in SEQ Equation * MERGEFORMAT . The designed burst pressure P_{burst} is based on a factor of safety FS and P_{max} as shown in SEQ Equation * MERGEFORMAT . The thickness of the tank walls $t_{tank_{RCS}}$ is determined by P_{burst}, r_{in}, yield strength of the material σ_Y, and FS as shown in SEQ Equation * MERGEFORMAT . The external volume of the tank $\forall_{ex}$ is dependent on r_{in} and $t_{tank_{RCS}}$ as shown in SEQ Equation * MERGEFORMAT . The dry mass of each tank $m_{tank_{dry_{fluid}}}$ is based on both $\forall_{in}$ and $\forall_{ex}$ as well as the density of the material of the tank $\rho_{mat_{RCS}}$ as shown in SEQ Equation * MERGEFORMAT . The wetted mass of each tank $m_{tank_{wet_{fluid}}}$ is the summation of $m_{tank_{dry_{fluid}}}$ and $m_{fluid_{tank}}$ as shown in SEQ Equation * MERGEFORMAT .

$$m_{fluid_{tank}} = \frac{2 m_{fluid}}{n_{RCS_{tank}}} \quad \text{Eq. 71}$$

$$\forall_{in} = \frac{m_{fluid_{tank}}}{\rho_{fluid}(1 - \delta_U)} \quad \text{Eq. 72}$$

$$r_{in} = \left(\frac{3\forall_{in}}{4\pi}\right)^{1/3} \quad \text{Eq. 73}$$

$$P_{max} = P_0 + \rho_{fluid} r_{in} G_{axial} g \quad \text{Eq. 74}$$

$$P_{burst} = P_{max} FS \quad \text{Eq. 75}$$

$$t_{tank_{RCS}} = \frac{P_{burst} r_{in} FS}{\sigma_Y} \quad \text{Eq. 76}$$

$$\forall_{ex} = \frac{4}{3}\pi\left(r_{in} + t_{tank_{RCS}}\right)^3 \quad \text{Eq. 77}$$

$$m_{tank_{dry_{fluid}}} = (\forall_{ex} - \forall_{in})\rho_{mat_{RCS}} \quad \text{Eq. 78}$$

$$m_{tank_{wet_{fluid}}} = m_{tank_{dry_{fluid}}} + m_{fluid_{tank}} \quad \text{Eq. 79}$$

The total volume $\forall_{tot}$ is the summation of the volumes of the fuel $\forall_{fuel}$ and oxidizer $\forall_{ox}$ with the number of tanks allocated for each accounted as shown in SEQ Equation * MERGEFORMAT . The mass of the helium pressurization system m_{He} is determined by scaling the summation of the dry tank mass of the fuel $m_{tank_{dry_{fuel}}}$ and the dry tank mass of the oxidizer $m_{tank_{dry_{ox}}}$ by 0.179279, a value that was obtained from an Aerojet Rocketdyne MEL as shown in SEQ Equation * MERGEFORMAT . Accounting for m_{He} and the summation of the dry tank masses, the total dry mass of the RCS system $m_{RCS_{dry}}$ is shown in SEQ Equation * MERGEFORMAT where it could be further simplified by scaling the dry mass summation without explicitly solving for m_{He}. The total wetted mass of the tanks $m_{RCS_{wet}}$ is the combination of the dry tank mass, fluid mass, and the helium pressurization system as shown in SEQ Equation * MERGEFORMAT . The piping mass $m_{RCS_{pipe}}$ is assumed to be 2% of $m_{RCS_{wet}}$ as shown in SEQ Equation * MERGEFORMAT . The mass of the thrusters $m_{RCS_{thrusters}}$ is simply the product of the mass of one thruster $m_{RCS_{thruster}}$ and the number of thrusters $n_{thrusters}$ as shown in SEQ Equation * MERGEFORMAT . The total mass of the RCS system m_{RCS} is the summation of the wetted mass of the tanks $m_{RCS_{wet}}$, $m_{RCS_{pipe}}$, and thrusters $m_{RCS_{thrusters}}$ as shown in SEQ Equation * MERGEFORMAT .

$$\forall_{tot} = \frac{n_{RCS_{tank}}}{2}\left(\forall_{fuel} + \forall_{ox}\right) \quad \text{Eq. 80}$$

$$m_{He} = 0.179279\frac{n_{RCS_{tank}}}{2}\left(m_{tank_{dry_{fuel}}} + m_{tank_{dry_{ox}}}\right) \quad \text{Eq. 81}$$

$$\begin{aligned} m_{RCS_{dry}} &= \frac{n_{RCS_{tank}}}{2}\left(m_{tank_{dry_{fuel}}} + m_{tank_{dry_{ox}}}\right) + m_{He} \\ &= 1.179279\frac{n_{RCS_{tank}}}{2}\left(m_{tank_{dry_{fuel}}} + m_{tank_{dry_{ox}}}\right) \end{aligned} \quad \text{Eq. 82}$$

$$m_{RCS_{wet}} = \frac{n_{RCS_{tank}}}{2}\left(m_{tank_{wet_{fuel}}} + m_{tank_{wet_{ox}}}\right) + m_{He} \quad \text{Eq. 83}$$

$$m_{RCS_{pipe}} = 0.02 m_{RCS_{wet}} \quad \text{Eq. 84}$$

$$m_{RCS_{thrusters}} = m_{RCS_{thruster}} n_{thrusters} \quad \text{Eq. 85}$$

$$m_{RCS} = m_{RCS_{wet}} + m_{RCS_{pipe}} + m_{RCS_{thrusters}} \quad \text{Eq. 86}$$

The power of the thrusters $\dot{W}_{RCS_{thrusters}}$ and piping $\dot{W}_{RCS_{pipe}}$ is determined by scaling the power of each thruster $\dot{w}_{RCS_{thruster}}$ and pipe $\dot{w}_{RCS_{pipe}}$ by $n_{thrusters}$ as shown in SEQ Equation * MERGEFORMAT and SEQ Equation * MERGEFORMAT , respectively.

$$\dot{W}_{RCS_{thrusters}} = \dot{w}_{RCS_{thruster}} n_{thrusters} \quad \text{Eq. 87}$$

$$\dot{W}_{RCS_{pipe}} = \dot{w}_{RCS_{pipe}} n_{thrusters} \quad \text{Eq. 88}$$

II.A.11 Solar Arrays

The solar array module has the required power to the loads during the daytime $\dot{W}_{req_{day}}$ as a single input. The outputs of this module are the masses of the array m_{array} and the mechanical components m_{mech}. It is assumed that the power required during the day for the loads is the same power required during the night as shown in Eq. (1). However, further work could show that additional power would be required during the night for heating the electrical components unless the heat rejected from CFM could be redirected to supply the required heat. The required power for the arrays $\dot{W}_{array}$ is based on the required power levels to the loads, the amount of time the spacecraft spends during the day T_d and during the night T_n, and the efficiencies of the power going through the batteries to the loads X_e and the power going to the loads directly while bypassing the batteries X_d as shown in Eq. (2). The mass of the array m_{array} is determined by the specific mass $m_{sp_{array}}$, $\dot{W}_{array}$, and the array mass margin M_{array} (in percent) as shown in Eq. (3). The masses of the other components such as the gimbal, release mechanism, and harness are determined using Eq. (4). Here, m_{tot_i} is the total mass of component i, m_i is the mass of a single component i, n_i is the number of i components, and M_i is the mass margin of component X. Using this, the total mass of the mechanical components is defined in Eq. (5) where k is the total number of the types of components.

$$\dot{W}_{req_{day}} = \dot{W}_{req_{night}} = \dot{W}_{req} \quad \text{Eq. 89}$$

$$\dot{W}_{array} = \frac{1}{T_d}\left(\dot{W}_{req_{day}} \frac{T_d}{X_d} + \dot{W}_{req_{night}} \frac{T_e}{X_e}\right) \quad \text{Eq. 90}$$

$$m_{array} = m_{sp_{array}} \dot{W}_{array} \left(1 + \frac{M_{array}}{100}\right) \quad \text{Eq. 91}$$

$$m_{tot_i} = m_i n_i \left(1 + \frac{M_i}{100}\right) \quad \text{Eq. 92}$$

$$m_{mech} = \sum_{i=1}^{k} m_{tot_i} = \sum_{i=1}^{k} m_i n_i \left(1 + \frac{M_i}{100}\right) \quad \text{Eq. 93}$$

II.B. Master Equipment List Integration

The master equipment list integration module combines the physics models of Section II.A and provides the spacecraft propellant mass, RCS propellant mass, structural mass, and propellant volume. The constants and specifications that are set for the physics models are read as a first step to this model which include over 100 parameters. The reader is advised to contact the lead author for more information on these values. The spacecraft mass, peak power draw, and

mass limited payload length are guessed with arbitrary values to start the calculations due to interdependencies. The order that the physics models are executed are as follows: Bus Structure, Docking Structure, Engine, Thrust Structure, Communications/Command & Data-Handling Systems/Guidance, Navigation, & Control, Main Propellant Tank, Reaction Control System, Cryogenic Fluid Management, Power Management and Distribution, and Solar Arrays. At this point, all the modules except for the Battery have been executed. The peak power draw is determined by the summation of all the power draws resulting from the outputs from all the executed physics modules and inputted into the Battery module. The mass of all the components is then summed and compared to that of the previous iteration. This repeats until convergence of the spacecraft mass.

II.C. Vehicle Input Card

The analysis begins with the vehicle card which has the Launch Vehicle (LV), mission burn specifications, and desired vehicle structure with the breakdown of drop, inline, and core stages as well as their propellant volume limitations based on launch vehicle limitations.

There are currently three stage types that are supported:

- **Drop Stage:** these stages are tanks that can be dropped as they empty throughout the mission. The propellant volume on these stages can be adjusted.
- **Inline Stage:** these stages cannot be dropped and serve as part of the vehicle structure. The propellant volume on these stages can also be adjusted.
- **Core Stage:** these stages contain the engines, and their propellant volume is not yet designed to be sized.

The LV configuration has LV selection options for each stage type which includes the drop, inline, and core stages along with the aggregation orbit that can all be specified:

- **Drop Stage LV:** Drop stage launch vehicle type
- **Inline Stage LV:** Inline stage launch vehicle type
- **Core Stage LV:** Core stage launch vehicle type
- **Orbit:** Aggregation orbit selection

The burn profile has four parameters that need to be specified:

- **Type:** Reaction Control System (RCS), Orbital Maneuvering System (OMS), and Main Burn
- **Name:** The name of each burn
- **ΔV:** The numerical value of the desired ΔV for the burn
- **Payload Adjustment:** The payload that is added/dropped AFTER the burn to account for crew members entering/exiting the vehicle, trash, samples, lander, etc.

Each stage has a set of two parameters that can be set:

- **Number of Stages**
- **Impose LV Volume Restrictions:** A Boolean parameter which will impose LV payload bay volume restrictions or just impose LV payload mass restrictions. LV mass restrictions are always imposed.

The payload stage is a special class of stage which only has one parameter, which is the initial payload mass. This mass includes structural components of the vehicle as well as the truss mass.

The engine block has three parameters:

- **Number of Engines**
- **Mass of Each Engine**
- **Engine Identifier (ID):** Once the psuedotransient dataset is populated for an engine configuration, this configuration shall have a unique ID which is the name of the .mat file which contains the makima splines of the engine parameters.

The RCS and OMS I_{sp} are set by the user as static values.

The main propellant has a set of five parameters:

- **Fluid:** a string array of propellant names that are used on the vehicle. At this point, the model can account for a bipropellant mixture such as hydrogen and oxygen. Future iterations could expand this to n number of propellants with specified mass or volume fractions.
- **Storage Temperature:** an array of temperatures at which the specified fluids are stored in the propellant tanks corresponding to their element number in the fluid string array.
- **Storage Pressure:** an array of pressures at which the specified fluids are stored in the propellant tanks corresponding to their element number in the fluid string array.
- **Mixture Ratio:** the fluid 1 to fluid 2 mass ratio. This is catered specifically towards a bipropellant engine. However, this could be expanded in future iterations to include mass fractions for n fluids specified in the fluid string array.
- **Cryogenic Fluid Management Configuration:** Can be set to either passive, active, or reduced boil-off.

The physics modules of Section II.A are executed according to the methodology of Section II.B for each stage type as initial guesses for the main Architecture model and saved into a Vehicle Card file. Table 2 through Table 9 show example inputs that will be used in this analysis.

Table 2: Launch Vehicle Selection

Parameter	Value
Drop Stage LV	New Glenn
Inline Stage LV	SLS 2B
Core Stage LV	SLS 2B
Orbit	Circular LEO

Table 3: Burn Profile

Parameter	Value	Units
Type of Burn	[RCS, OMS, Main, Main, OMS, Main, Main, RCS, OMS]	-
Name of Burn	{'LDRO to LDHEO (RCS)', 'LDRO to LDHEO (OMS)', 'TMI', 'MOI','Plane Changes (OMS)', 'TEI', 'EOI', 'LDHEO to LDRO (RCS)', 'LDHEO to LDRO (OMS)'}	-

ΔV of Burn	[66, 93, 1289, 3055, 50, 1800, 1096, 66, 93]	m/s
Payload Adjustment After the Burn	[0, -328, 989, 9435, 0, -995,328, 0, 0]	kg

Table 4: Payload

Parameter	Value	Units
Payload Initial Mass	48000	kg

Table 5: Drop Stages

Parameter	Value	Units
Number of Stages	6	-
Volume Limit	300	m^3
RCS Initial Mass	260	kg
Structural Mass	8726.5	kg

Table 6: Inline Stages

Parameter	Value	Units
Number of Stages	1	-
Volume Limit	905.5	m^3
RCS Initial Mass	5782	kg
Structural Mass	13118	kg

Table 7: Core Stages

Parameter	Value	Units
Number of Stages	1	-
Volume Limit	627.144	m^3
RCS Initial Mass	700	kg
Structural Mass	15720	kg

Table 8: Engine Block

Parameter	Value	Units
Number of Engines	2	-
Engine Mass	5000	kg
Engine ID	‘hydrogen_NTP_530MW_even_TP’	kg

Table 9: Propellant(s)

Parameter	Value	Units
RCS	329	s
OMS	450	s
Main Propellant	[“Hydrogen”]	-
Storage Temperature	[20]	K

Storage Pressure	[202650]	Pa
Mixture Ratio	-	-

II.D. Simulation Setup Inputs

The simulation setup is a set of user defined inputs that define the optimization that the system will perform:

- **Results Folder:** The folder into which the results will be saved at the end of the simulation.
- **Flight Performance Reserve:** The percentage of ΔV that is added to the desired ΔV to provide margin.
- **Ramp Limit Type:** The type of ramp limit to which the engine block will evaluate and adhere as the pseudotransient database is evaluated. Currently, reactor power $\frac{\mathrm{d}\dot{Q}}{\mathrm{dt}}$ and fuel temperature $\frac{\mathrm{d}T_f}{\mathrm{dt}}$ are supported.
- $\frac{\mathbf{dX}}{\mathbf{dt}}$**:** The numerical temporal derivative values for the ramp rate.
- **Parameter to Adjust:** This is the parameter that is desired to be adjusted with the following options:
  - *Propellant volume:* Adjust the propellant volume to adhere to the mission ΔV.
  - *ΔV:* Adjust the ΔV for a given propellant volume
  - *None:* Run the mission with the current vehicle configuration. This type of analysis does not undergo iterations.
- **Stage to Adjust:** This parameter selects stage type of which the number of stages will be adjusted with the following options:
  - *Drop*
  - *Inline*
  - *None:* The number of stages remains the same, but the volume limit will be violated if the propellant volume required exceeds this limit.
- **Jettison Tank Type:** The tanks that are to be jettisoned as they empty with the following options:
  - *Drop*
  - *Inline*
- **Number of Simultaneous Tank Jettisons:** The number of tanks to drop simultaneously to prevent cantilever effects. This parameter can be any positive integer.
- **Tolerance:** The error tolerance between each iteration as a percentage. This defines when the simulation meets the convergence criteria.
- **Time Step:** The simulation time step. This is important for accurate representation of transient performance and plays a role in the resolution used in the convergence criteria.
- **Maximum Burn Iterations:** This is the maximum number of iterations that occur per burn when the burn time is adjusted to account for transient effects to meet the ΔV requirements.
- **Maximum Vehicle Convergence Iterations:** The maximum total number of iterations for the model to evaluate before stopping the simulation. This is used to avoid an infinite

number of iterations in case the model finds an oscillation point. When this occurs, either the time step and/or tolerance should be adjusted.

- **Proportional Exponent:** This exponent is used on the proportional controller to adjust the specified parameter to adjust.
- **Reaction Control System (RCS) Adjustment Flag:** This is a Boolean value that is used to turn on and off the mass adjustment of the RCS propellant to meet the RCS burn ΔV requirements.
- **RCS Tolerance:** This is the mass value within which the RCS mass is deemed to be converged. This is used when the RCS Adjustment Flag is set to be true.

Table 10 shows an example with the inputs and their values.

Table 10: Example Architecture Model Inputs

Parameter	Value/Argument	Units
Results Folder Name	'Opposition_2033_6_engines'	-
Flight Performance Margin	4	%
Ramp Limit Type	'dQ_dt'	-
$\frac{dX}{dt}$	[18,-18]	MW/s
Parameter to Adjust	'Volume'	-
Stage to Adjust	'Drop'	-
Jettison Tank Type	'Drop'	-
Number of Simultaneous Tank Jettisons	2	-
Tolerance	0.5	%
Time Step	0.1	s
Maximum Burn Iterations	20	-
Maximum Vehicle Convergence Iterations	100	-
Proportional Exponent	0.5	-
RCS Adjustment Flag	1	-
RCS Tolerance	10	kg

II.E. RCS and OMS Burns

The Architecture model will read the Vehicle Card and iterate through all the burns listed on it. Both RCS and OMS burns use the Ideal Rocket Equation to determine the propellant mass used to achieve the desired ΔV as shown in Eq. 94.

$$m_{prop\,used} = \left(m_{dry} + m_{RCS} + m_{prop}\right)\left[1 - \exp\left(-\frac{\Delta V}{I_{sp}}\right)\right] \qquad \text{Eq. 94}$$

II.F. NTP Burns

II.D.1 Decay Heating

The NTP burns use the psuedotransient data base from the specified engine ID to perform transient burns with the incorporation of point kinetics and decay heating using Eq. 95 with the constant parameters specified in Table 11 taken from BWXT's analysis.

$$\dot{Q}_{decay}(t) = \dot{Q}_{avg}\left\{\frac{\rho}{\rho-\beta}\exp\left(\frac{\rho-\beta}{\Lambda}t\right) - \frac{\beta}{\rho-\beta}\exp\left(\frac{-\rho\lambda}{\rho-\beta}t\right) + 0.1104\left[t^{-0.2436} - \left(t_{fp}+t\right)^{-0.2436}\right]\right\} \quad \text{Eq. 95}$$

Table 11: Neutronics Constants

Constant	Symbol	Given Values
Fission Yield	β	0.0065 --
Decay Constant	λ	0.0764 s^{-1}
Prompt Neutron Lifetime	Λ	6×10^{-5} s
Reactivity	ρ	-0.01377 \$

II.D.2 NTP Engine Transients

Based on the temporal derivative $\frac{dX}{dt}$ criteria, the engine transient performance is evaluated. It is important to note that all parameters in the psuedotransient database are functions of $\dot{Q}$. In any case, the transient calculation starts from power level of the previous iteration $\dot{Q}_{i-1}$ and aims to obtain a desired power level $\dot{Q}_{des}$. For powering up, $\dot{Q}_{des}$ is set to the reactor full power and for powering down, $\dot{Q}_{des}$ is set to the idle power level which is 7 kWt from SNP specifications where the residual reactor heat can be dissipated through radiation alone. From the $\frac{dX}{dt}$ criteria, the parameter X that is to be ramped at iteration i, or X_i, is evaluated at $\dot{Q}_{i-1}$ and at $\dot{Q}_{des}$ to yield X_{i-1} and X_{des}, respectively. The $\frac{dX}{dt}\Delta t$ is added to X_{i-1} to yield X_i. Should X_i evaluate to a value that is beyond X_{des}, then X_i is set to be equal to X_{des}. This provides a constant ramp rate for X from which $\dot{Q}_i$ is obtained. Since decay heating is considered, Eq. 3.5 is evaluated and $\dot{Q}_{decay}$ is added to $\dot{Q}_i$ such that $\dot{Q}_i = \dot{Q}_i + \dot{Q}_{decay}$. Based on the new $\dot{Q}_i$, all other parameters are evaluated using makima interpolation of the psuedotransient parameters. At each iteration, the burn time t is incrementally increased by Δt and the evaluated parameters at each iteration are recorded in an array which includes the engine thrust F and mass flow rate $\dot{m}$.

II.D.3. Vehicle Performance

During each iteration, the propellant mass m_{prop_i} is calculated by subtracting $\dot{m}\Delta t$ from $m_{prop_{i-1}}$. The total vehicle mass is calculated by $m_{tot_i} = m_{prop_i} + m_{RCS} + m_{dry}$. Furthermore, ΔV_i is calculated from the average total vehicle mass between iterations $i-1$ and i by $\overline{m}_{tot_i} = \frac{m_{tot_{i-1}} + m_{tot_i}}{2}$ and applying the thrust of all the engines $n_{engines}F$ on the engine block through Newton's second law or $\Delta V_i = \Delta V_{i-1} + \frac{n_{engines}F}{\overline{m}_{tot_i}}$.

II.G. Architecture Model Iterations

The Architecture Analysis Code reads the Vehicle Card as well as user specified optimization parameters and criteria and performs the analysis. After the analysis is completed,

the code creates a specified folder with transient burn profile graphs illustrating the vehicle and engine performance parameters as well as a breakdown of the vehicle performance of each burn and resulting optimized vehicle structure in a spreadsheet.

II.G.1. Vehicle Performance Iterations

The vehicle performance convergence schemes have three options which include: (1) converging on a set ΔV by changing the propellant volume, (2) converging on a set propellant volume by changing the total vehicle ΔV and reducing the ΔV of each burn by the same fractional amount, and (3) performing no convergence and simply running the last burn until the propellant mass is zero. At each iteration, the integrated MEL is executed to determine if the selected launch vehicles can support the new stage masses, if not, then additional stages are added. The code also checks if the number of stages can be reduced and try to maximize the launch vehicle effectiveness.

The convergence scheme used is a modified proportional controller shown in Eq. 96 where Y_{des} is the desired value of the dependent variable, Y_i is the value of the dependent variable at the i^{th} iteration, X_i is the value of the independent variable at the i^{th} iteration, and X_{i+1} is the new value or guess for the independent variable. The α parameter is the proportional exponent used in the stability of the convergence. A higher α could result in faster convergence, however, it could result in a divergent solution as well. A lower α results in longer computational time but is generally more stable than a higher α. Once the relative error between Y_i and Y_{des} is less than the tolerance, the model is said to be converged.

$$X_{i+1} = X_i \left(\frac{Y_i}{Y_{des}} \right)^{\alpha} \qquad \text{Eq. 96}$$

II.G.2. Vehicle Performance Iterations

After each burn is performed, the model checks to see if enough propellant was expelled to correspond to the propellant volume occupied by the number of empty stages to be jettisoned at the same time. Should the stages be jettisoned, the dry mass and any remaining RCS mass in those stages are removed from the vehicle mass allocations for the rest of the iteration. Similarly, during vehicle performance convergence and the adjustment of the propellant volume as the independent parameter, if the resulting X_{i+1} is greater than the propellant volume that can be contained in all of the stages when their volume limits are assumed, then the same number of tanks that are to be dropped at a time will be added to the vehicle along with their dry mass and RCS mass. Moreover, if X_{i+1} results in a propellant volume lower than the total propellant volume without the first tanks to be jettisoned, then the number of tanks to be jettisoned decreases by the user specified number of tanks to jettison at a time.

III. COPERNICUS GRAVITY LOSSES

A suite of Copernicus decks was created for use in tandem with the architecture sizing model to investigate gravity losses. Gravity losses are defined as the additional impulse, in excess of that required for an impulsive burn, required by a spacecraft to achieve a targeted v_∞. This additional impulse is required due to the engine burning on-axis with the nearby planet's gravitational vector. In Figure 1, the red lines represent the engine burn vector. This figure demonstrates how the burn does not occur directly perpendicular to the gravity vector, as in an ideal impulsive burn at periapsis. Spacecraft with low thrust to weight ratios are particularly susceptible to these effects, as they require a longer burn time to accelerate to the required velocity

and therefore are accelerating against the gravitational pull for a longer period. To facilitate rapid iteration, four separate Copernicus decks were created.

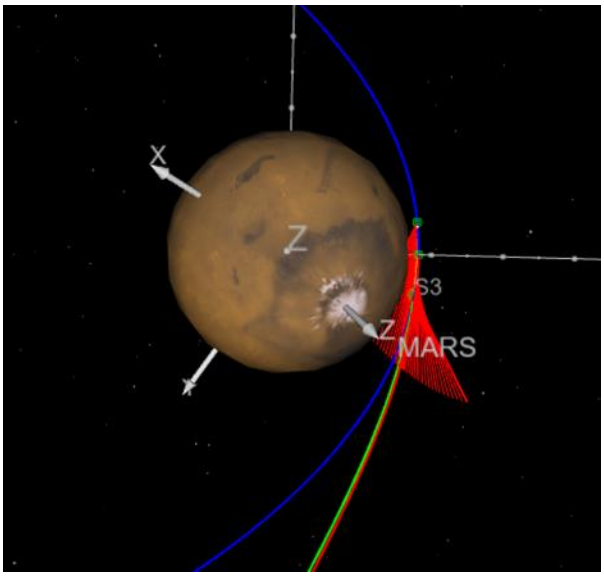

Figure 1: Reference Mars Opposition Class Vehicle

By decoupling each burn, the convergence process was much easier between iterations. Each burn was verified with test cases. One deck was created for each major NTP burn:

- TMI: Trans-Mars Insertion
- MOI: Mars Orbit Insertion
- TEI: Trans-Earth Insertion
- EOI: Earth Orbit Insertion

The gravity loss Copernicus decks worked as follows:

1. The reference mission's impulsive delta-v is input
2. Spacecraft parameters are input (this can be T/W ratio, specific wet masses, or even desired burn times)
3. Copernicus determines the v∞ achieved by the impulse burn
4. Copernicus solves for a finite burn resulting in the same v∞ as the impulse burn

A python script was utilized to converge several missions at once, with the resulting gravity losses being iterated through the architecture vehicle sizing model until convergence was reached.

For the reference 2039 Opposition class mission, the additional percentage of ΔV required to mitigate the gravity losses $\%\Delta V_{loss_X}$ are estimated to follow the curves presented in Eq. 97 through Eq. 100 for the TMI, MOI, TEI, and EOI burns, respectively, as functions of the thrust to weight ratio of the aggregated vehicle at each burn. Notice that the DSM is not included in this list since it is assumed that gravity losses will be minimal. Furthermore, these equations are mission specific and will change from mission to mission.

$$\%\Delta V_{loss_{TMI}} = 0.0004\left(\frac{F_{tot}}{m_{tot}}\right)^{-1.702} \quad \text{Eq. 97}$$

$$\%\Delta V_{loss_{MOI}} = 0.0006\left(\frac{F_{tot}}{m_{tot}}\right)^{-1.81} \quad \text{Eq. 98}$$

$$\%\Delta V_{loss_{TEI}} = 0.0009\left(\frac{F_{tot}}{m_{tot}}\right)^{-1.9} \quad \text{Eq. 99}$$

$$\%\Delta V_{loss_{EOI}} = 0.0005\left(\frac{F_{tot}}{m_{tot}}\right)^{-1.73} \quad \text{Eq. 100}$$

IV. Results and Discussion

The thrust to weight analysis with gravity losses aims to determine the optimum number of engines at the extreme cases of Mars opposition class total mission ΔV of 7.5 km/s for 2033 and 10.5 km/s for 2039. From Copernicus modeling, it was determined that gravity losses are about 2.5% per 1000 seconds of burn time. This means that there should be a propellant mass savings when the thrust to weight ratio of the vehicle increases. The thrust to weight ratio of the vehicle was varied by modifying the number of NTP engines with the assumption that each engine has a mass of 5000 kg consistent with SNP's estimations. The baseline vehicle was assumed to be Aerojet Rocketdyne's Opposition class vehicle shown in

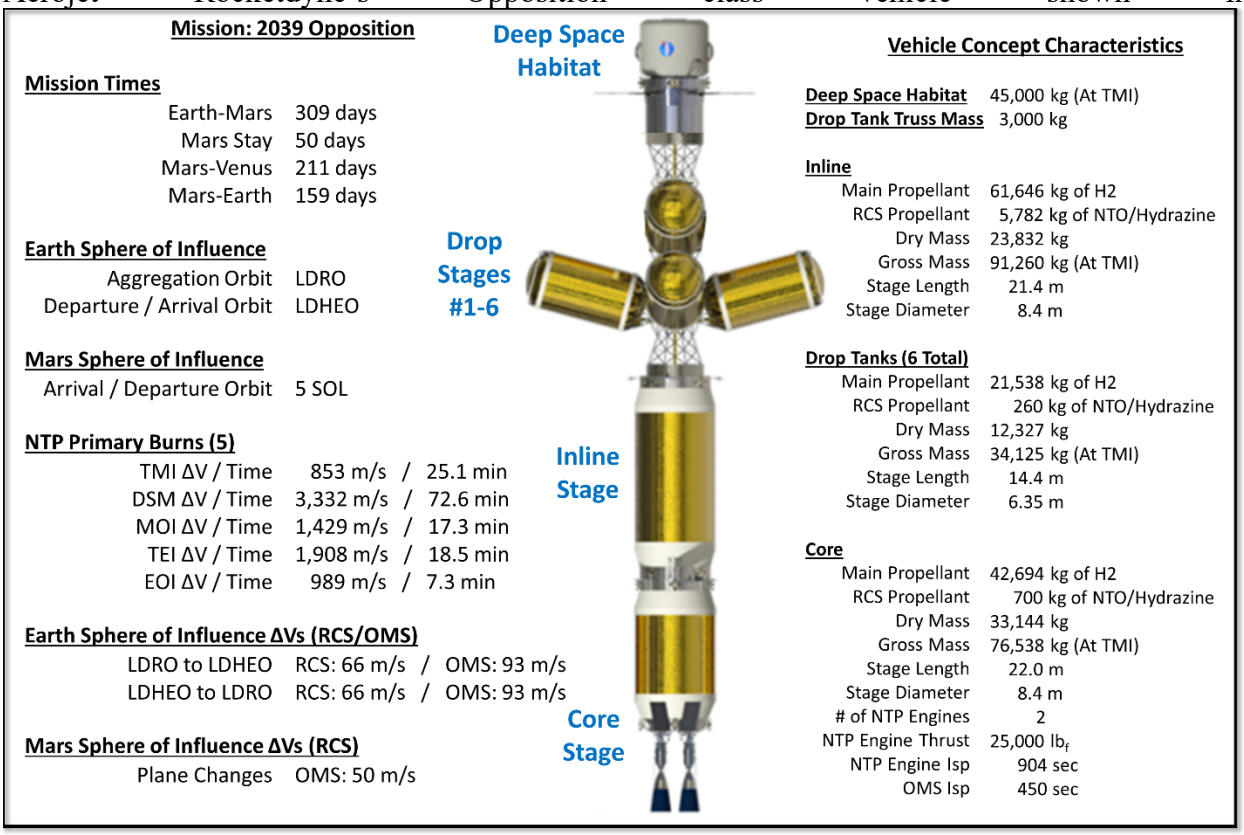

Figure **2**. Here, the vehicle features drop tanks that are jettisoned as they empty.

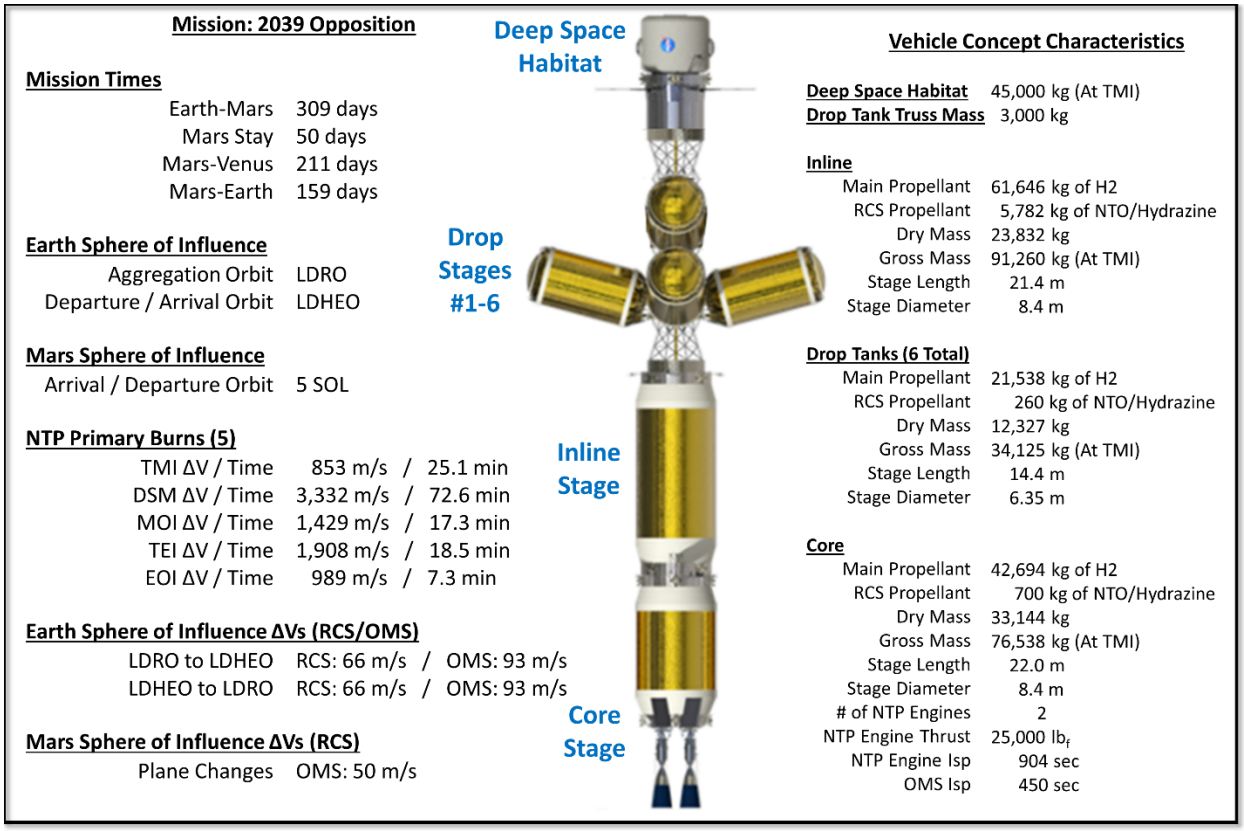

Figure 2: Reference Mars Opposition Class Vehicle
Credit: NASA/Aerojet Rocketdyne

Two iterations were examined by adjusting the ΔV of each burn in accordance with the resulting burn time and Table 12 and Table 13 show the results. Since the ΔV of the 2033 mission is lower than that of the 2039 mission, the burn times of the 2033 mission are significantly lower than that of the 2039 mission. Furthermore, both missions feature a decrease in both ΔV and burn time as the number of engines is increased as shown in Table 12. However, since the vehicle dry mass increases with an increased number of engines, the total initial vehicle mass also increases which includes the propellant tanks as well as the number of jettison tanks. This is true for both the 2033 and 2039 missions which suggests that higher gravity losses are beneficial from the point of view of the vehicle mass. However, other factors may play a role in decision making as longer burn times also impact the engine reliability and decrease the total number of burns/missions that the engine block can support.

Table 12: ΔV and Burn Durations

Burn Name	2033 2X Engines		2033 4X Engines		2033 6X Engines		2039 2X Engines		2039 4X Engines		2039 6X Engines	
	ΔV (m/s)	Duration (s)	ΔV (m/s)	Duration (s)	ΔV (m/s)	Duration (s)	ΔV (m/s)	Duration (s)	ΔV (m/s)	Duration (s)	ΔV (m/s)	Duration (s)
TMI	1384.8	2342.5	1332.1	1208.7	1315.0	901.4	2298.2	10921.7	2049.4	5217.8	2048.1	3925.9
MOI	3345.6	3915.6	3221.6	2035.3	3158.7	1432.4	1313.7	4077.7	1261.0	2178.3	1260.3	1634.6
TEI	1850.0	1209.1	1818.2	662.0	1810.0	490.1	6219.3	10916.6	5963.7	5965.0	5960.7	4510.3
MOI	1146.0	633.6	1116.0	349.4	1137.7	266.7	1714.0	968.9	1733.5	553.7	1698.0	400.3

Table 13: Vehicle Parameters

Parameter	2033 2X Engines	2033 4X Engines	2033 6X Engines	2039 2X Engines	2039 4X Engines	2039 6X Engines
# Drop Tanks	6	6	8	30	32	36
# Inline Stages	1	1	1	1	1	1
Total Propellant Mass (mton)	225.79	236.41	257.24	742.54	772.4	872.73
Total RCS Mass (mton)	10.28	10.86	12.2	26.56	28.18	31.4
Total Dry Mass (mton)	168.04	179.39	209.52	443.54	474.81	532.54
Total Vehicle Mass (mton)	404.1	426.66	478.96	1212.64	1275.39	1436.67

The same analysis was performed for the ammonia-based engines.

V. CONCLUSION

This section will be filled out in the final version of the paper.

ACKNOWLEDGMENTS

This work was supported by NASA's Space Technology Mission Directorate (STMD) through the Space Nuclear Propulsion (SNP) project. This work was funded under Contract No. 80LARC23DA003.

REFERENCES

[1] Robbins, W. H., and Finger, H. B., "An Historical Perspective of the NERVA Nuclear Rocket Engine Technology Program," NASA Contractor Report NASA-CR-187154, Analytical Engineering Corporation, July 1991.

[2] Nikitaeva, D., and Thomas, D. L., "Alternative Propellant Nuclear Thermal Propulsion Engine Architectures," *Journal of Spacecraft and Rockets*, 2022, pp. 1–11. https://doi.org/10.2514/1.A35289

[3] "Thermophysical Properties of Fluid Systems," National Institute of Standards and Technology (NIST), 2022.

[4] Nikitaeva, D., and Dale Thomas, L., "Impacts of In Situ Alternative Propellant on Nuclear Thermal Propulsion Mars Vehicle Architectures," *Journal of Spacecraft and Rockets*, Vol. 59, No. 6, 2022, pp. 2038–2052. https://doi.org/10.2514/1.A35399

[5] Williams, J., Senent, J. S., Ocampo, C., and Davis, E. C., "Overview and Software Architecture of the Copernicus Trajectory Design and Optimization System," presented at the 4th International Conference on Astrodynamics Tools and Techniques, Madrid, Spain, 2010.

[6] Nikitaeva, D., Smith, C. D., and Duchek, M., "Engine Cycle Comparison for Alternative Propellant Nuclear Thermal Propulsion Engines," presented at the ASCEND 2023, Las Vegas, Nevada, 2023. https://doi.org/10.2514/6.2023-4715

[7] Duchek, M. E., Nikitaeva, D., Harnack, C., Grella, E., and Greenhalge, S., "Parametric Modeling of NTP Engine Performance for a Crewed Mars Mission," presented at the ASCEND 2023, Las Vegas, Nevada, 2023. https://doi.org/10.2514/6.2023-4717